Korean J. Chem. Eng., **31**(12), 2157-2161 (2014)
DOI: 10.1007/s11814-014-0170-8

pISSN: 0256-1115
eISSN: 1975-7220

Precursor effect on catalytic properties of Mo-based catalyst for sulfur-resistant methanation

Haiyang Wang*, Zhenhua Li*,†, Baowei Wang*, Xinbin Ma*,†, Shaodong Qin, Shouli Sun**, and Qi Sun****

*Key Laboratory for Green Chemical Technology of Ministry of Education, School of Chemical Engineering and Technology, Tianjin University, Tianjin 300072, China
**National Institute of Clean-and-Low-Carbon Energy, Beijing 102209, China
(*Received 28 March 2014 • accepted 19 June 2014*)

Abstract−The catalytic activity of Mo-based catalysts prepared from $(NH_4)_6Mo_7O_{24}$ and $(NH_4)_2MoS_4$ was compared in the sulfur resistant methanation process. The catalyst using oxide precursor had relatively higher activity than the catalyst using sulfide precursor, and the presulfidation procedure almost had no effect on the catalytic performance of the catalyst using oxide precursor. In view of the characterization results, it could be supposed that the amorphous MoS_2 was more active for sulfur-resistant methanation than the crystalline MoS_2. The molybdenum sulfides and oxides with lower valence states (Mo^{4+}, Mo^{5+}) could be responsible for the catalytic activity and make a possible contribution to the carbon monoxide methanation in the reaction condition.

Keywords: Sulfur-resistant, Methanation, Precursor, Active Species

INTRODUCTION

The production of substitute natural gas (SNG) from coal or biomass is good for relieving the problem of greenhouse gas emission and the energy crisis. Methanation is the key step which needs to be achieved with catalyst [1,2]. Ni-based catalyst is generally applied for the methanation reaction as follows:

$$3H_2+CO \rightarrow CH_4+H_2O \quad (1)$$

In former methanation literatures, the Ni-based catalysts usually show high conversion of CO when they react with hydrogen-rich feed ($H_2/CO>3$) and low reaction temperature (<400 °C). But because the syngas produced from gasifier is the mixture in a H_2/CO mole ratio from 0.3 to 1.3 which is low for good CO conversion, so the water gas shift process ($CO+H_2O \leftrightarrow CO_2+H_2$) is needed before methanation step to enhance the H_2/CO mole ratio close to 3. Moreover, a sulfur species removal process such as rectisol wash is crucial before methanation due to the restrictions of sulfur-sensitive catalyst like Ni-based catalyst. These processes increase the cost of SNG production on Ni-based catalyst. For these reasons, Mo-based catalysts have received much attention for their insensitivity to sulfur poisoning [3,4] and their tolerance to outlet gases from gasifiers with low H_2/CO ratios [5,6] although they have only modest activity. It is possible for Mo-based catalyst to cover the shortage of relatively lower activity by using simplified production technology. The methanation reaction occurring on Mo-based catalyst is described as follows:

$$2CO+2H_2 \rightarrow CH_4+CO_2 \quad (2)$$

The above reaction is the sum of a methanation (1) and water gas shift reaction, which can be achieved because the water gas shift reaction activity on Mo-based catalyst is much higher than that on Ni-based catalyst. All the sour species (H_2S, CO_2, etc.) can be removed in one-step operation after methanation process. By this way, the SNG production from coal or biomass can be achieved in a shorter process on Mo-based catalyst than that on the Ni-based catalyst.

Ammonium heptamolybdate (AHM) was a commonly used precursor to prepare supported Mo-based catalyst, and a sulfidation process was normally needed to activate this kind of catalyst. For this kind of catalyst, $Al_2(MoO_4)_3$ species could be formed on the catalyst surface and result in decreased reaction activity [7,8]. As reported, ammonium tetrathiomolybdate (ATM) decomposed in inert gas can directly lead to a nonstoichiometric MoS_2 formation [9], which has been successfully used in the hydrodesulfurization studies. Some results indicate that the catalyst prepared by decomposition of ATM has a higher activity than the conventional catalyst prepared from AHM [10,11].

Previous studies and density functional theory calculations showed that low valence sulfur species located on the MoS_2 edges were supposed to be involved in H_2 activation [12,13]. CO was found to adsorb on the bridge position of the Mo-edge of a MoS_2 surface with a tilted configuration, and it was unlikely to dissociate into O and C [14]. Some C_1 species may be acceptable for the hydrogenation of CO adsorbed on the coordinatively unsaturated molybdenum sites of MoS_2 clusters [15,16]. However, to our knowledge, there is no related report concerning the active sites on sulfur-resistant methanation catalysts. In this work, we investigate the difference of $(NH_4)_6Mo_7O_{24}$ or $(NH_4)_2MoS_4$ as precursor in methanation activity and discuss the effect of precursor in this process.

EXPERIMENTAL

1. Catalyst Preparation

ATM ($(NH_4)_2MoS_4$) was self-made by adding a 20 wt% aque-

†To whom correspondence should be addressed.
E-mail: zhenhua@tju.edu.cn, xbma@tju.edu.cn

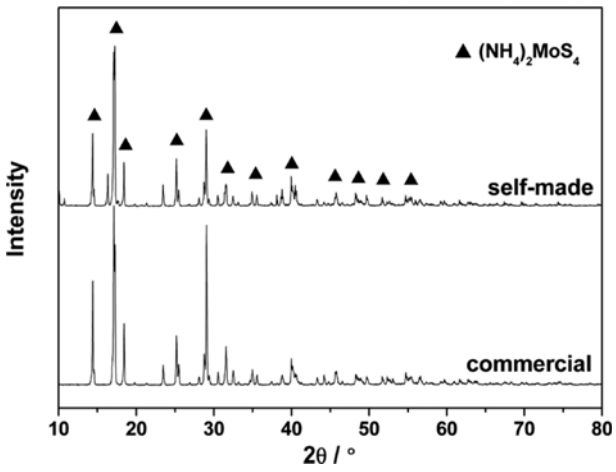

Fig. 1. XRD patterns of $(NH_4)_2MoS_4$.

ous solution of $(NH_4)_2S$ to a solution of AHM ($(NH_4)_6Mo_7O_{24}$) and $NH_3 \cdot H_2O$ upon stirring at room temperature. The mixture was stirred and heated moderately at 60 °C for 1 h, then kept in a refrigerator for 24 h. The precipitated dark red crystals of ATM were filtered and washed with cold ethanol, followed by drying under vacuum. The characteristic X-ray diffraction (XRD) peak positions and relative intensities of self-made sample clearly corresponded to a commercial product from Alfa Aesar with purity of 99.99% metal basis (Fig. 1).

The γ-Al_2O_3 support used in this study is commercially available (Yixing, China). The molybdenum oxide sample was prepared by the incipient wetness impregnation method with an aqueous solution of AHM. After impregnation for 24 h, the obtained sample was dried in air at 120 °C for 12 h and then calcined at 600 °C for 4 h. This catalyst was designated as MoOAl. The molybdenum sulfide sample was prepared by impregnation of the support with an aqueous solution of ATM. The obtained sample was dried in inert gas at 60 °C and then stored in a desiccator under nitrogen atmosphere. This catalyst was designated as MoSAl. All above catalysts were prepared with the same loading of Mo (10 wt%).

2. Activity Test

Activity tests were carried out in a fixed-bed reactor (700 mm length and 11 mm diameter) with three independent electric heating zones to ensure the isothermal region was larger than 10 cm in the middle part. The temperature in each zone was controlled by individual thermocouple and the reaction temperature was measured with another thermocouple placed in the middle of the catalyst bed. In this way, the temperature gradient along the catalyst bed was controlled less than 10 °C in the experiment we tested. The reaction temperature in the paper means the hot-spot temperature, which was determined by moving the thermocouple along the catalyst bed during reaction. As for the radial temperature gradient, we think it can be neglected because the inner diameter of the reactor tube is as small as 11 mm.

Prior to the catalyst test, the as-prepared catalyst (3 mL, 20-40 mesh) was activated in the reactor under different condition at atmospheric pressure. The catalyst MoSAl was calcined in nitrogen at 400 °C for 5 h, and the catalyst MoOAl was sulfurized by a 3 vol% H_2S/H_2 gas mixture at 400 °C for 5 h. As a comparison, MoOAl without pre-sulfidation was also investigated.

The syngas, at a flow rate of 250 mL/min (volume ratio of N_2 : CO : H_2=1 : 2 : 2, with 0.2 vol% H_2S), was introduced to the reactor. The reaction pressure was 3 MPa. The exit gases were on-line analyzed using an Agilent 7890A gas chromatography instrument. The composition of CO, CO_2, CH_4, and C_2H_6 was obtained using external standard method based on gas chromatography analysis results.

3. Characterization

N_2-physisorption analysis of the prepared catalysts was performed at 196 °C on a Tristar-3000 apparatus (Micromeritics, America) to obtain the textural properties of catalysts. XRD analysis was performed using a Rigaku D/max-2500 X-ray diffractometer with a Ni-filtered Cu-Kα radiation source (λ=1.54056 Å). The morphology and structure of the catalysts were characterized by a JEM-2100F (200 kv) transmission electron microscope (TEM) with a high resolution of 0.15 nm/200 kv. X-ray photoelectron spectroscopy (XPS) analysis of all catalyst samples was performed using PHI-1600 ESCA XPS equipment with monochromated Mg-Kα X-ray radiation.

RESULTS AND DISCUSSION

1. Comparison of Methanation Activity

Under experimental conditions with 0.2 vol% H_2S, methanation activities of the two catalysts are presented in Fig. 2. Each point in

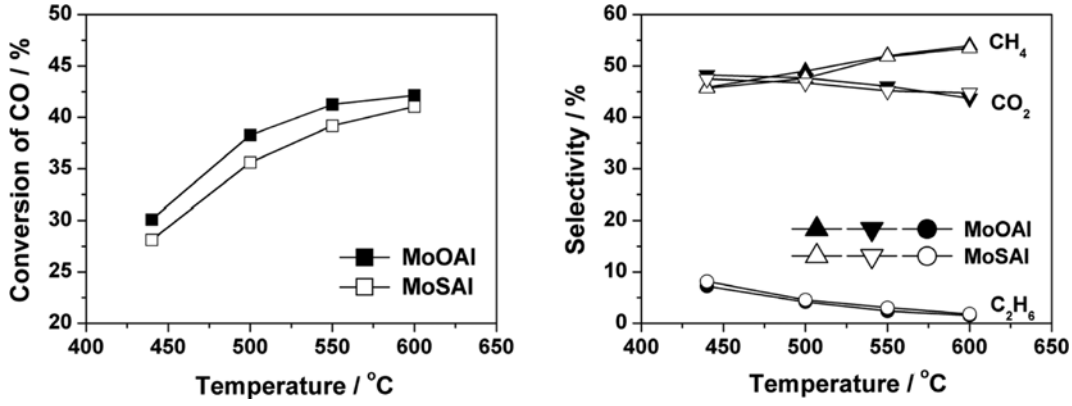

Fig. 2. Methanation activity of catalysts prepared from different precursors.

Table 1. Textural property of catalysts after test

Catalyst	BET surface area, m^2/g	Pore volume, cm^3/g	Pore size, nm
MoOAl	150	0.22	5.4
MoSAl	159	0.20	4.3

the figure is the average of two hours data after an eight hour test. The results indicated that the catalysts increased their CO conversion with increasing reaction temperature. As reaction temperature increased, CH_4 selectivity increased while CO_2 selectivity decreased, and C_2H_6 selectivity decreased at a low level. It was clear that the MoSAl catalyst prepared from ATM exhibited a lower CO conversion than the MoOAl from AHM. However, there was no difference in the selectivity of any product.

In previous studies [17,18], Mo-based methanation catalysts were reported to have significant activity with CO conversion about 60% at relatively lower space velocity (800-2,000 h^{-1}). In our paper, the space velocity (5,000 h^{-1}) is relatively higher than those reported. To some extent, our results progressed compared with reported results.

2. Analysis of Catalyst Property

The textural properties of used catalysts are shown in Table 1. It is observed that data of the catalysts are similar to each other. This indicates that AHM and ATM had comparable effect on the textural properties of Al_2O_3 support. The difference of pore size could be attributed to the larger grain size of MoS_2 on catalyst MoSAl.

The phase identification of used catalysts was performed by means of X-ray diffraction techniques (Fig. 3). It is clear that the γ-Al_2O_3 structure (broad peaks, 2θ of 32.8°, 37.0°, 45.8°, 59.9° and 66.8°) are present on the two catalysts. $Al_2(MoO_4)_3$ phase was not detected before monolayer coverage was achieved [19]. On catalyst MoSAl, the peaks corresponding to MoS_2 (2θ of 14.4° and 40.0°) proved the existence of a considerable amount of crystalline MoS_2. But no diffraction peaks of MoS_2 were detected on MoOAl, which meant that the molybdenum sulfides were highly dispersed on this catalyst surface. So the predominant molybdenum species of MoOAl in test were amorphous or microcrystalline MoS_2, relatively rich in

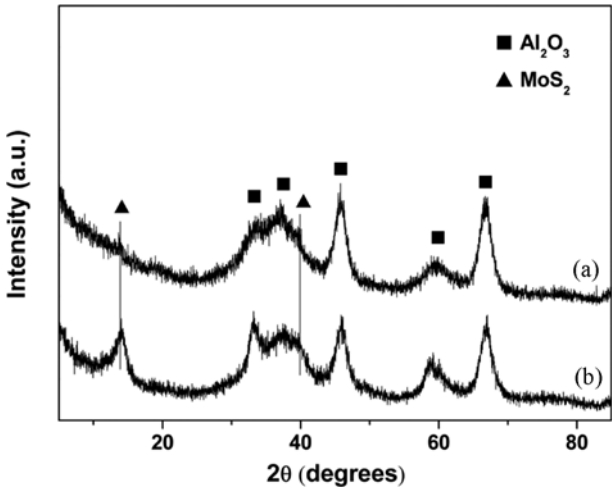

Fig. 3. The XRD patterns of catalysts after activity test: (a) MoOAl, (b) MoSAl.

defects. These phases could provide more active sites for CO adsorption on the Mo-edge of a MoS_2 surface [20].

The TEM analysis shown in Fig. 4 was used to further determine the structural features of MoS_2 on the used catalysts. The image of catalyst MoSAl displayed a well crystallized MoS_2 stack with more layers in contrast to that of MoOAl with bent MoS_2 slabs and fewer layers. To compare quantitatively the distribution of slab length and stacking after methanation reaction, statistical analyses were made based on the analysis of about 10 images and 100 slabs located in various parts of the each same catalyst. The slab length distribution of Mo/Al and Co-Mo/Al catalysts is presented in Fig. 5 The average length and stacking number of MoS_2 particles calculated from the TEM images are summarized in Table 2.

Many single slabs were present on MoOAl, indicating a slab-alumina interaction which is stronger than the slab-slab interaction. And the smaller slab could provide more edge active sites. The slab-like structure contained defects like curvatures, dislocations, substitution of sulfur by oxygen [21]. This meant that molybdenum spe-

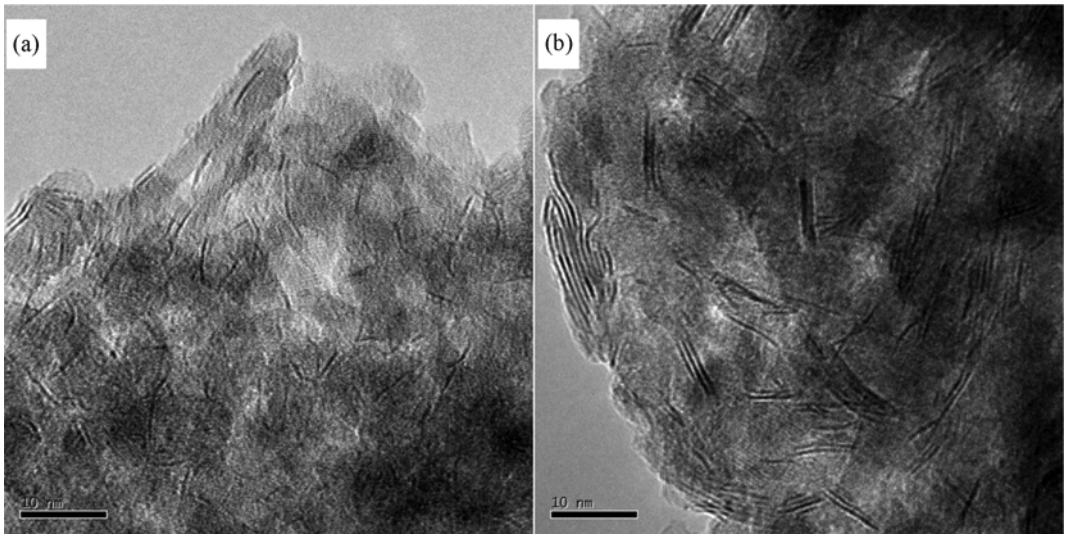

Fig. 4. The TEM images of catalysts after activity test: (a) MoOAl, (b) MoSAl.

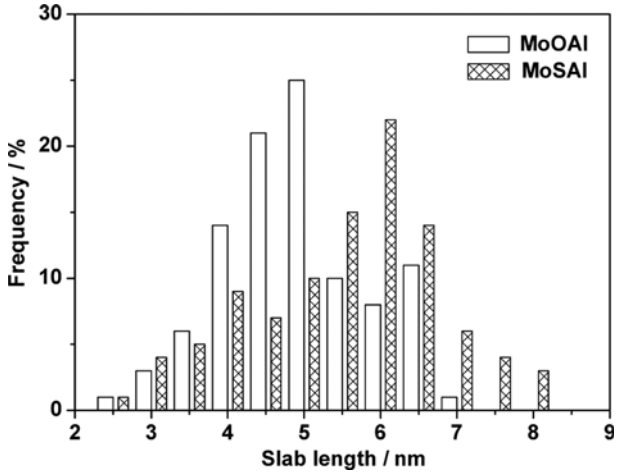

Fig. 5. Distribution of slab length for MoOAl and MoSAl catalyst.

cies might have different valence states in the tests.

To know the chemical state and the distribution of Mo on the carrier, XPS analysis was carried out to characterize the used catalysts. It is obvious in Fig. 6 that the binding energy regions of Mo3d and S2s overlap with each other. For the deconvolution of the Mo 3d peaks, the following constraints were imposed: the spin-orbit splitting of the Mo 3d peaks was fixed to be around 3.2. The area ratios were equal to the theoretical values of 1.5. The decomposition of Mo 3d spectra represented three types of Mo species: sulfides (Mo^{4+}), oxides (Mo^{6+}) and oxysulfides (Mo^{5+}), which are well documented [22,23]. Their peak positions and area ratios are listed in Table 3.

As O-S exchange occurred easily by reaction of Mo oxide with H_2S at low temperature, the molybdenum phase on used catalysts

Table 2. The average slab length (L) and stacking (n) of the MoS_2 slabs on catalysts

Catalyst after treatment	Average slab length, nm	Average stacking degree
MoOAl	4.9	1.0
MoSAl	5.5	2.6

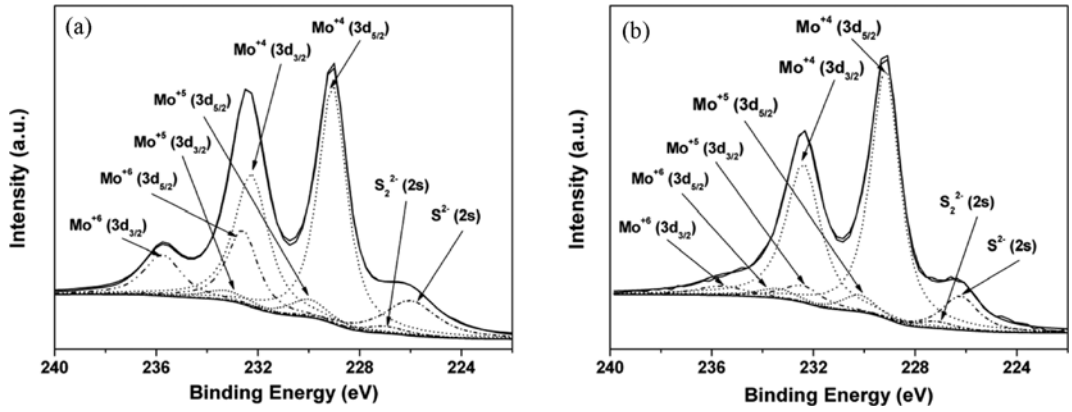

Fig. 6. Peak-fitting of Mo3d-S2s XPS peaks for the used catalysts: (a) MoOAl, (b) MoSAl.

Table 3. XPS parameters derived from curve fitting of Mo3d–S2s

Catalyst	S/Mo	Binding energy, eV			Quantitative result, %atom		
		Mo^{+4} $3d_{5/2}$	Mo^{+5} $3d_{5/2}$	Mo^{+6} $3d_{5/2}$	Mo^{4+}	Mo^{5+}	Mo^{6+}
MoOAl	1.85	229.1	230.0	232.6	69.4	7.1	23.5
MoSAl	2.01	229.2	230.2	232.4	85.3	6.6	08.1

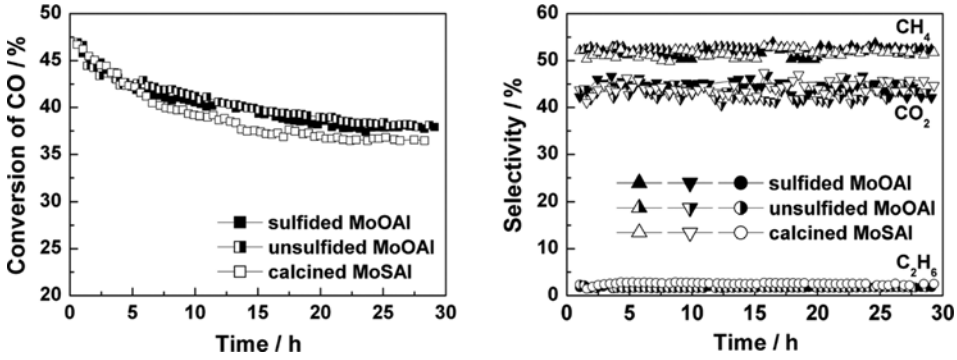

Fig. 7. Methanation activity over time at 550 °C for different samples.

should be mainly the species with lower valence. For catalyst MoSAl, the higher percentage of sulfide phase (Mo^{4+}) was in agreement with previous observations. The intermediate, presumably a MoO_xS_y species, was attributed to some oxygen atoms on γ-Al_2O_3 support occupied sulfur positions. For catalyst MoOAl, the higher percentage of MoO_x (Mo^{6+}) was partly due to un-sulfurizable molybdenum oxides and partly due to re-oxidation of the sample exposure to air and water during storage or transfer [24].

3. Evaluation of Active Species

To study the molybdenum species responsible for the catalytic performance, methanation activities over time for catalyst MoOAl were compared at 550 °C in the presence and absence of H_2S. Also evaluated was a MoOAl sample without sulfidation. The curves in Fig. 7 show that the presulfidation process might not be essential for this kind of catalyst in methanation. No obvious differences were detected in the results of these samples. CO conversion decreased at the initial reaction stage, including subsequent relatively stable conversion rate. Stable selectivities of products were achieved on all samples.

As MoO_3 was found to be easily reduced by hydrogen to Mo_4O_{11}, MoO_2 and Mo metal at temperature higher than 400 °C [25], molybdenum was definitely in the oxide form with lower valence on the sample after reaction in the absence of H_2S, showing molybdenum oxide had similar methanation activity with the molybdenum sulfide. Some oxysulfide intermediates could be assumed to have methanation activity under the reaction conditions.

CONCLUSIONS

The catalyst prepared from AHM exhibited better methanation activity than the catalyst prepared from ATM, through increasing the dispersion of Mo species on the catalyst surface, diminishing the MoS_2 size and providing more active sites. The amorphous MoS_2 phase was more active for methanation than the highly crystalline MoS_2 phase. Also, molybdenum oxide showed a similar activity to the molybdenum sulfide. So, molybdenum sulfides and oxides with lower valence could be all active species in methanation process, and AHM was better as a precursor than ATM even without the presulfidation treatment.

ACKNOWLEDGEMENTS

The authors gratefully acknowledge financial support from the National Institute of Clean and Low-Carbon Energy (NICE) and from Tianjin Municipal Science and Technology Commission (14JCZDJC 37500).

REFERENCES

1. J. Kopyscinski, T. J. Schildhauer and S. M. A. Biollaz, *Fuel*, **89**, 1763 (2010).
2. W. R. Kang and K. B. Lee, *Korean J. Chem. Eng.*, **30**, 1386 (2013).
3. H. Farag, K. Sakanishi, M. Kouzu, A. Matsumura, Y. Sugimoto and I. Saito, *Catal. Commun.*, **4**, 321 (2003).
4. M. Y. Kim, S. B. Ha, D. J. Koh, C. Byun and E. D. Park, *Catal. Commun.*, **35**, 68 (2013).
5. Y. Cao, Z. Y. Gao, J. Jin, H. C. Zhou, M. Cohron, H. Y. Zhao, H. Y. Liu and W. P. Pan, *Energy Fuel*, **22**, 1720 (2008).
6. M. Logan, A. Gellman and G. A. Somorjai, *J. Catal.*, **94**, 60 (1985).
7. N. Rinaldi, T. Kubota and Y. Okamoto, *Appl. Catal. A*, **374**, 228 (2010).
8. B. W. Wang, G. Z. Ding, Y. G. Shang, J. Lv, H. Y. Wang, E. D. Wang, Z. H. Li, X. B. Ma, S. D. Qin and Q. Sun, *Appl. Catal. A*, **431-432**, 144 (2012).
9. D. G. Kalthod and S. W. Weller, *J. Catal.*, **95**, 455 (1985).
10. P. T. Vasudevan and S. W. Weller, *J. Catal.*, **99**, 235 (1986).
11. P. T. Vasudevan and F. Zhang, *Appl. Catal. A*, **112**, 161 (1994).
12. S. Cristol, J. F. Paul, E. Payen, D. Bougeard, S. Clémendot and F. Hutschka, *J. Phys. Chem. B*, **106**, 5659 (2002).
13. X. D. Wen, T. Zeng, B. T. Teng, F. Q. Zhang, Y. W. Li, J. G. Wang and H. J. Jiao, *J. Mol. Catal. A*, **249**, 191 (2006).
14. J. C. Muijsers, T. Weber, R. M. Van Hardeveld, H. W. Zandbergen and J. W. Niemantsverdriet, *J. Catal.*, **157**, 698 (1995).
15. Y. L. Fu, X. B. Tang, Z. G. Huang, C. Z. Fan, M. R. Ji and J. X. Wu, *Appl. Catal.*, **55**, 11 (1989).
16. X. R. Shi, H. J. Jiao, K. Hermann and J. G. Wang, *J. Mol. Catal. A*, **312**, 7 (2009).
17. P. Y. Hou and H. Wise, *J. Catal.*, **93**, 409 (1985).
18. R. C. Zhu, *Mod. Chem. Ind.*, **32**, 33 (2012).
19. D. S. Zlngg, L. E. Makovsky, R. E. Tlscher, F. R. Brown and D. M. Hercules, *J. Phys. Chem.*, **84**, 2898 (1980).
20. M. Huang and K. Cho, *J. Phys. Chem. C*, **113**, 5238 (2009).
21. P. J. Kooyman, E. J. M. Hensen, A. M. De Jong, J. W. Niemantsverdriet and J. A. R. Van Veen, *Catal. Lett.*, **74**, 49 (2001).
22. T. K. T. Ninh, L. Massin, D. Laurenti and M. Vrinat, *Appl. Catal. A*, **407**, 29 (2011).
23. L. M. Qiu and G. T. Xu, *Appl. Surf. Sci.*, **256**, 3413 (2010).
24. P. J. Kooyman and J. A. R. Van Veen, *Catal. Today*, **130**, 135 (2008).
25. T. Ressler, R. E. Jentoft, J. Wienold, M. M. Günter and O. Timpe, *J. Phys. Chem. B*, **104**, 6360 (2000).